Ductile-Brittle Transition in Martensitic 12%Cr Steel

V. Dudko*, J. Borisova and R. Kaibyshev

Belgorod State University, Pobeda 85, Belgorod 308015, Russia

Mechanical behavior of a 12Cr–0.6Mo–2.2W–4Co–0.8Cu-VNb steel was studied by tension and the Charpy impact tests in the temperature range of 133–473 K. The yield stress and uniform elongation increase concurrently with decrease of temperature because of the work-hardening rate tends to increase with decrease of temperature. At temperatures below 213 K, the steel exhibits a poor-defined yield plateau. Impact tests demonstrate that the ductile-brittle transition occurs at 323 K. The impact toughness value comprises 250 J/cm^2 at $\geq$ 373 K. The impact toughness decreases to 100 J/cm^2 at room temperature. The steel becomes completely brittle at 273 K, when the absorbed energy falls to 8 J/cm^2. Fracture mechanisms in 12Cr–0.6Mo–2.2W–4Co–0.8Cu-VNb steel are discussed.

1. Introduction

High Cr martensitic steels possess high creep resistance, adequate corrosion and oxidation resistance at exploitation conditions [1–3]. The high creep resistance is achieved by a complex alloying that provides solution and dispersion strengthening of tempered martensite lath structure, which itself also contributes to increase in strength because of the internal stresses inherent in martensite [1, 4–6]. The steels with 9%Cr are especially tough when tempered and exhibit a low ductile-brittle transition temperature (DBTT) [7–10]. The creep strength and oxidation resistance should be improved, concurrently, for further increase in service temperature of these steels [1–3]. Oxidation resistance is extremely important for high Cr steels used for steam turbine blades. Chromium is the most effective alloying element to improve oxidation resistance [2, 3]. However, increase of chromium content above 10% may result in the formation of δ-ferrite which is a detrimental phase for creep strength and fracture toughness [8]. As a result, at room temperature, the steel may become brittle and prone to cracking especially under dynamic loading condition. Impact toughness is important issue for reliability of 9%Cr steels used for boiler tube and main steam pipes and critically important property for 12%Cr used for turbine blades.

The aim of the current study is to examine ductile-brittle transition in advanced 4%Co and 0.8%Cu modified 12%Cr steel. Specific attention is paid to examination of origin and nature of embrittlement of this steel and role of alloying in toughness. To achieve this goal, the mechanical behavior of this steel was examined at low and elevated temperatures by tension test and the Charpy impact testing.

2. Experimental

The steel with a chemical composition of Fe - 0.1 ĐĄ - 11.9 Cr - 4.0 Co - 0.8 Cu - 0.59 Mo - 2.2 W - 0.22 V - 0.05 Nb - 0.065 Ni - 0.05 Si - 0.05 Mn - 0.008 B - 0.012 N (in mass%) was fabricated by Central Research Institute for Machine-Building Technology, Moscow, Russia. This steel was normalized at 1343 K for 40 min and then tempered at 1043 K for 3 h. Tensile specimens with a cross-section of 7×3 mm^2 and a gauge length of 35 mm were deformed in tension at temperatures ranging from 133 to 293 K using an Instron 5882 mechanical testing machine equipped with an Instron SFL 3119-408 environmental chamber. Standard Charpy V-notch specimens were tested using an Instron 450 J impact machine (Model SI-1M) at temperatures ranging from 253 to 373 K. The percent shear fracture was measured in accordance with the ASTM E-23 standard [11].

Structural characterizations were carried out using an Olympus GX71 optical microscope (Olympus LTD, Japan), a JEM-2100 (JEOL Ltd., Tokyo, Japan) transmission electron microscope (TEM) equipped with an INCA energy dispersive X-ray spectroscope (Oxford Instruments, Oxfordshire, UK). Surface of the specimen for metallography observations was mechanically polished and then chemically etched in a solution of 2%HNO$_3$+1%HF +97%H$_2$O. Foils for TEM studies were prepared by double-jet electropolishing using a solution of 10% perchloric acid in glacial acetic acid. The lath/subgrain sizes were measured from TEM micrographs by the linear intercept method, including all clearly visible (sub)boundaries. The dislocation densities were evaluated by counting the individual dislocations in the grain/subgrain interior, and each data point represents at least six arbitrarily selected representative TEM images.

Chemical composition of ferrite was calculated with version 5 of the Thermo-Calc software using the TCFE7 database.

*corresponding author; e-mail: valeriy_dudko@yahoo.com

3. Results

3.1. Microstructure after tempering

The microstructures of the steel after quenching and tempering are shown in Fig. 1. Tempered martensite lath structure is dominant; volume fraction of δ-ferrite is 3.8% (Fig. 1a). Average size of prior austenite grain (PAG) is $\approx 38\ \mu$m (Fig. 1a). δ-ferrite having a "bamboo" shape [8] locates at boundaries of PAGs and packets as continuous shell. Lath thickness is 286 nm; high dislocation density of $2.2 \times 10^{14}\ \mathrm{m}^{-2}$ is observed within laths (Fig. 1b). Particles of $M_{23}C_6$ carbides and MX carbonitrides have very small dimensions. $M_{23}C_6$ carbides with an average size of ≈ 83 nm locate at boundaries of PAGs, packets,

blocks and laths (Fig. 1b). The MX carbonitrides with an average dimension of ≈ 7 nm and plate-like shape precipitated within ferritic matrix (Fig. 1c).

3.2. Tensile properties

Typical engineering stress–strain curves measured at different temperatures are shown in Fig. 2. The values of yield stress (YS), S_y, ultimate tensile strength (UTS), S_u, uniform elongation, El_u, and total elongation, El_t, are summarized in Table I. Static mechanical properties of the martensitic 12 pct Cr steel correlate with those of P92-type steel [7]. The shapes of the engineering stress–strain curves are approximately the same in the temperature range of 133–293 K. Continuous yielding is observed at $T \geq 213$ K. At lower temperatures, transition to discontinuous yielding takes place; poor-defined yield plateau followed by work hardening stage could be distinguished. Prolonged uniform plastic deformation is provided by a noticeable strain hardening which becomes stronger with decrease of temperature. Both strength and uniform ductility tend to increase with decreasing temperature at $T \geq 153$ K. At 133 K, ductility decreases, insignificantly. No evidence for DBT could be found in tension. The steel is ductile down to 133 K.
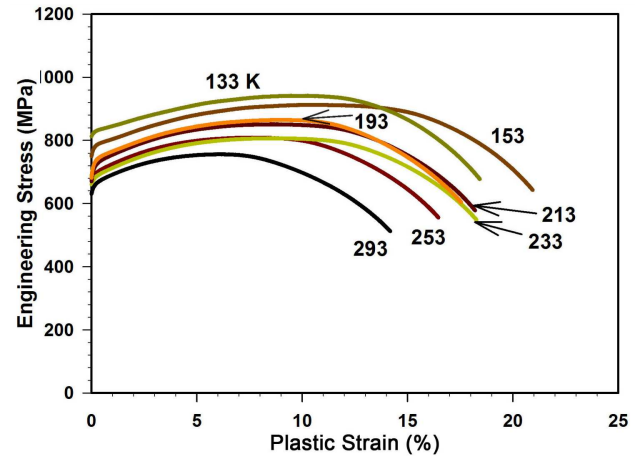
Fig. 2. Engineering curves at different temperatures.

TABLE I

Static mechanical properties of a 12 pct Cr martensitic steel at different temperatures.

Parameters	Temperature [K]						
	133	153	193	213	233	253	293
S_y [MPa]	829	782	734	720	684	696	661
S_u [MPa]	1033	1009	944	922	877	869	803
S_f [MPa]	1395	1319	1257	1246	1193	1211	1139
El_u [%]	9.8	10.6	9.2	8.5	8.8	7.5	6.1
El_t [%]	18.4	20.9	17.5	18.2	18.2	16.4	14.2

3.3. Impact tests

The Charpy V-notch impact-absorbed energy and a portion of the shear fracture of the 12%Cr steel are presented in Fig. 3. V-notch impact absorbed energies at upper and lower shelf were estimated to be 250 and 9 J/cm^2,
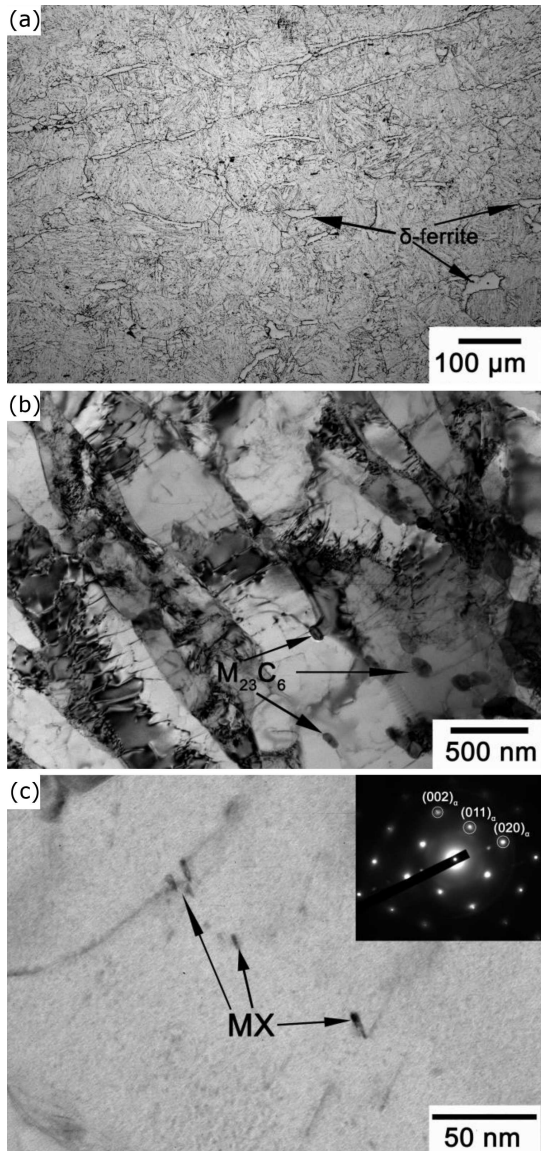
Fig. 1. Microstructure of a 12 pct Cr martensitic steel after tempering at 1043 K for 3 h: (a) optical photograph, (b) tempered martensite lath structure and (c) MX carbonitrides within laths.

respectively. The DBTT of ≈ 311 K was considered to be the temperature corresponding to impact energy absorption halfway between the upper and lower shelf energies of the steel. This temperature corresponds to the appearance of the 50% ductile fracture on the surface of the impact specimen and therefore the fracture appearance transition temperature (FATT) and DBTT are the same. At 293 K below the DBTT, the steel possesses a high value of absorbed energy of 110 J/cm^2, and the absorbed energy then falls to 9 J/cm^2 at a temperature of 253 K.
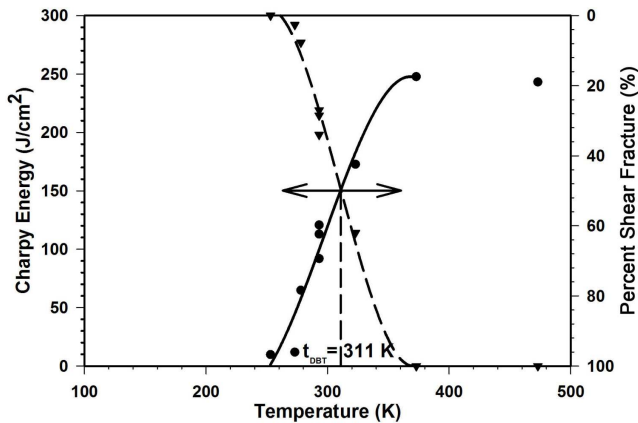

Fig. 3. Temperature dependence of the Charpy energy and the percent of shear fracture in 12 pct Cr martensitic steel.

Metallography observations showed limited number of secondary cracks in V-notch Charpy impact specimens fractured at ambient temperature (Fig. 4). At room temperature, the fracture surface consists of the initiation zone (IZ), the fibrous zone (FZ), the unstable zone (UZ) and the shear lips zone (SLZ) (Fig. 4a). Figure 4b shows profile of crack propagation across IZ and FZ. The stable crack propagation in the FZ occurs in an essentially ductile manner. A large ductile region with elongated grains and large voids within ferritic matrix are observed. Preferential cracks or voids nucleation in δ-ferrite grains were not found. Figure 4c shows the cleavage fracture propagation unit in a brittle-fracture profile corresponding to the UZ. Crack propagation occurs by transgranular cleavage mechanism. It can be seen that the brittle crack deflects at block and PAG boundaries. Secondary cracks are observed in ferritic matrix, mainly.

Figure 5 shows fracture surfaces of impact specimen tested at a temperature of 253 K. Fracture surface consists of IZ and UZ (Fig. 5a). The onset of unstable crack propagation occurs after very short initiation stage and occurs through transgranular cleavage mechanism (Fig. 5b). There are a lot of secondary crack beneath the fracture surface. These cracks are initiated at large particles of $M_{23}C_6$ located on PAG boundaries (Fig. 5b).

Fig. 5. Fracture surface in the Charpy V-notch specimen of a 12 pct Cr martensitic steel tested at temperature of 253 K: macrograph view (a), optic profile view of unstable zone (b).
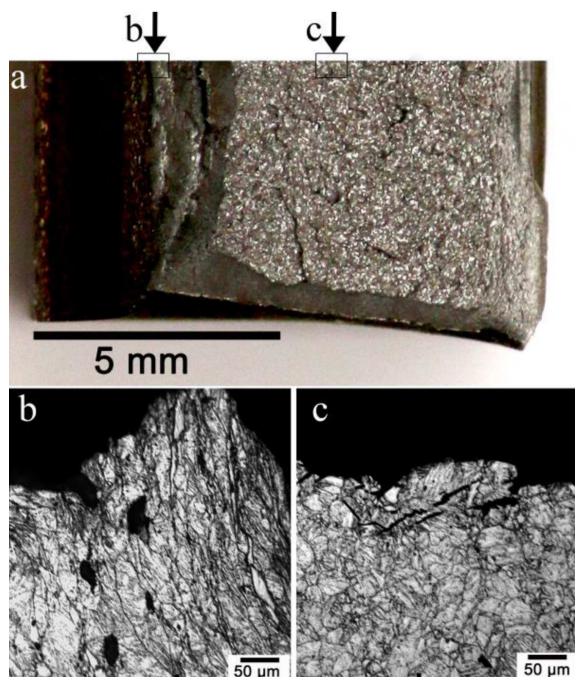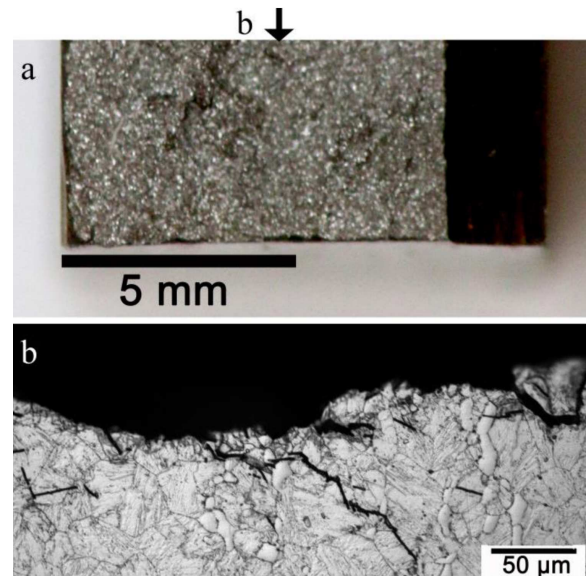

Fig. 4. Fracture surface in the Charpy V-notch specimen of a 12 pct Cr martensitic steel tested at room temperature: macrograph view (a), optic profile view of initiation and fibrous zones (b), optic profile view of unstable zone (c). Framed regions in figure (a) indicate places locations of b, and c.

4. Discussion

Inspection of experimental data shows that 12Cr–0.6Mo–2.2W–4Co–0.8Cu-VNb steel remains highly tough and ductile under static tension up to a temperature of 133 K. However, the steel becomes fully brittle at temperature of 253 K under V-notch Charpy impact test. It is

well known that the yield strength increases rapidly with decrease of temperature, while fracture stress is independent of temperature. The fracture is accompanied by plastic deformation at the temperature region when the fracture stress is higher than the yield strength, because the yielding occurs first. In the temperature range in which the fracture stress is lower than the yield strength, the cleavage fracture occurs before plastic deformation. No premature fracture occurs because a high energy is necessary for the formation of a macrocrack with critical dimension susceptible for unstable propagation in tension. In addition, there exists a difference between static and dynamic strain rates in the tension test $(10^{-3}$ s$^{-1})$ and the impact test $(\approx 10^3$ s$^{-1})$. Flow stresses in tensile tests are much lower than those in the impact ones due to lower strain rate and lacking notch root on the smooth tensile specimens. However, values of fracture stresses are nearly the same under static and dynamic loadings. Thus the fracture of tensile specimen occurs after remarkable plastic strain. In V-notch impact test the already created flaw plays the role of crack with critical size susceptible to unstable propagation at $T \leq 253$ K.

The DBTT in the martensitic 12%Cr steel is remarkably higher (by 100 K) than that in martensitic 9%Cr steels [7]. No obvious differences in the distributions and sizes of second phase particles could be found in the studied martensitic 12%Cr steel and P92-type steel. Moreover, dimensions of boundary $M_{23}C_6$ carbides and MX carbonitrides located in ferritic matrix are significantly lower. Laths microstructures in both steels were also similar. The main difference between microstructures is a presence of δ-ferrite in the microstructure and increased Cr content and Co additions. It is believed that the secondary carbides forming along the $\delta-$ ferrite grain boundaries are larger than those in the tempered martensite matrix. These larger secondary carbides provide favorable places for critical microcracks to nucleate and hence the DBTT is degraded [10]. However, preferential cracks or voids nucleation in δ-ferrite grains were not found in our work. These results indicate that the decrease in DBTT cannot be explained by the formation of δ-ferrite shell, grain size and precipitates. It has been supposed, consequently, that the decrease in DBTT of the 12%Cr steel is attributed to addition of 3%Cr and 4%Co that leads to decreased toughness of ferrite matrix due to short-range ordering. This may be a reason why the toughness of the steel strongly depends on chromium and cobalt content in solid solution. In the future, the role of chromium and cobalt solutes and the optimum concentration of these alloying elements will be revealed in detail.

5. Conclusions

1. The 12%Cr steel exhibits no embrittlement under static tension. Strength and ductility increase with decrease of temperature, concurrently. At 153 K, transition from continuous yielding to discontinuous one occurs with decreasing temperature. At 153 K, the elongation-to-failure of $\approx 21\%$ is higher than that at ambient temperature.

2. The impact toughness of the 12%Cr steel with the addition of 4%Co decreases from 250 J/cm^2 to 9 J/cm^2 with decreasing temperature from 373 to 253 K. The ductile-brittle transition temperature is 311 K. The steel exhibits a relatively high impact toughness of 100 J/cm^2 at a temperature of 293 K.

References

[1] R. Viswanathan, W. Bakker, *JMEPEG* **10** 81 (2001).

[2] R. Viswanathan, J. Sarver, J.M. Tanzosh, *JMEPEG* **15**, 255 (2006).

[3] P.J. Ennis, W.J. Quadakkers, in: *Creep Resistant Steels*, Eds. F. Abe, T.-U. Kern, R. Viswanathan, Woodhead Publ., Cambridge, UK 2008, p. 519.

[4] F. Abe, as Ref. [3], p. 279.

[5] V. Dudko, A. Belyakov, R. Kaibyshev, *ISIJ Int.* **57**, 540 (2017).

[6] V. Dudko, A. Belyakov, R. Kaibyshev, *MSF* **706-709**, 841 (2012).

[7] V. Dudko, A. Fedoseeva, R. Kaibyshev, *Mater. Sci. Eng. A* **682**, 73 (2017).

[8] F. Abe, P. Araki, N. Noda, *Mater. Sci. Tech.* **8**, 762 (1992).

[9] A. Chatterjee, D. Chakrabarti, A. Moitra, R. Mitra, A.K. Bhaduri, *Mater. Sci. Eng. A* **630**, 58 (2015).

[10] K.J. Harrelson, S.H. Rou, R.C. Wilcox, *J. Nucl. Mater.* **141-143**, 508 (1986).

[11] ASTM E23-05, Standard test methods for notched bar impact testing of metallic materials, *Annual Book of ASTM Standards*, 03.01, ASTM International, Pennsylvania, USA 2005.